

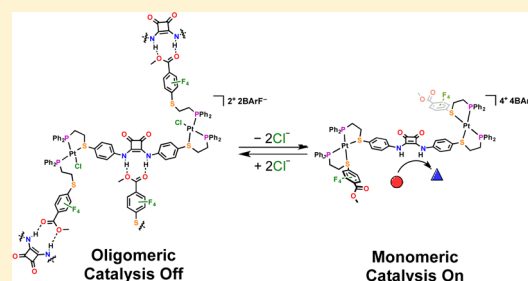
Allosteric Regulation of Supramolecular Oligomerization and Catalytic Activity via Coordination-Based Control of Competitive Hydrogen-Bonding Events

C. Michael McGuirk, Jose Mendez-Arroyo, Alejo M. Lifschitz, and Chad A. Mirkin*

Department of Chemistry and The International Institute for Nanotechnology, Northwestern University, 2145 Sheridan Road, Evanston, Illinois 60208-3113, United States

Supporting Information

ABSTRACT: Herein, we demonstrate that the activity of a hydrogen-bond-donating (HBD) catalyst embedded within a coordination framework can be allosterically regulated in situ by controlling oligomerization via simple changes in coordination chemistry at distal Pt(II) nodes. Using the halide-induced ligand rearrangement reaction (HILR), a heteroligated Pt(II) triple-decker complex, which contains a catalytically active diphenylene squaramide moiety and two hydrogen-bond-accepting (HBA) ester moieties, was synthesized. The HBD and HBA moieties were functionalized with hemilabile ligands of differing chelating strengths, allowing one to assemble them around Pt(II) nodes in a heteroligated fashion. Due to the hemilabile nature of the ligands, the resulting complex



can be interconverted between a flexible, semiopen state and a rigid, fully closed state in situ and reversibly. FT-IR spectroscopy, ¹H DOSY, and ¹H NMR spectroscopy titration studies were used to demonstrate that, in the semiopen state, intermolecular hydrogen-bonding between the HBD and HBA moieties drives oligomerization of the complex and prevents substrate recognition by the catalyst. In the rigid, fully closed state, these interactions are prevented by steric and geometric constraints. Thus, the diphenylene squaramide moiety is able to catalyze a Friedel–Crafts reaction in the fully closed state, while the semiopen state shows no reactivity. This work demonstrates that controlling catalytic activity by regulating aggregation through supramolecular conformational changes, a common approach in Nature, can be applied to man-made catalytic frameworks that are relevant to materials synthesis, as well as the detection and amplification of small molecules.

INTRODUCTION

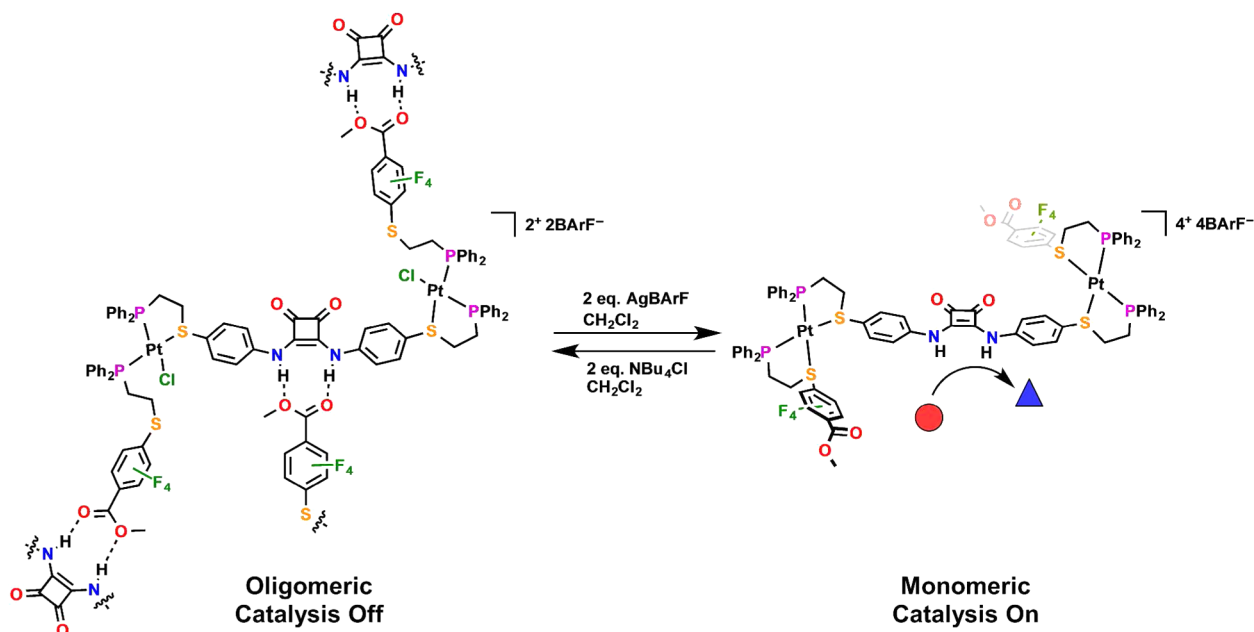
In over 40 distinct metabolically active enzymes, allosteric up-regulation of catalytic activity is characterized by the dissociation of dormant higher-order enzyme oligomers into catalytically active dimers or monomers.¹ Previous to up-regulation, the active site of such enzymes can participate in the formation of higher order quaternary structures via hydrogen-bonding interactions, forming tertiary peptide structures at the active site that impede substrate recognition, and thus catalytic activity.^{2,3} Like other allosteric mechanisms, the dissociation of dormant oligomers is regulated by the binding of small-molecule “effectors” to chemically orthogonal recognition sites on the enzyme.⁴ Oligomer dissociation not only exposes the enzymatic face containing the active site, but also causes conformational changes in the tertiary structure of the active site, alleviating catalytically detrimental hydrogen bonds between key amino acids. The resulting hydrogen-bonding network of the active site is then able to recognize and activate an electrophilic substrate, initiating catalytic turnover. Inspired by the role of hydrogen-bonding in the quaternary and tertiary structures of such allosterically regulated enzymes, we set out to design an analogous coordination-based system in which the reversible binding of small-molecule effectors regulates hydro-

gen-bond-driven oligomerization, substrate recognition, and catalytic activity. By developing a novel methodology for the allosteric regulation of catalytically active coordination-based complexes, we open the door to applications in small-molecule detection and amplification, as well as multicomponent cascade reactions. Using the weak-link approach (WLA) to the synthesis of coordination-driven supramolecular structures, we embedded both hydrogen-bond-donating (HBD) and hydrogen-bond-accepting (HBA) moieties within a coordination framework.^{5,6} In these complexes, recognition of coordinating small-molecule analytes at distal Pt(II) centers is followed by conformational changes in the supramolecular structure, thereby allosterically regulating the ability of the hydrogen-bonding pairs to form intermolecular, catalytically deactivating interactions (Scheme 1).

Among the various methodologies for synthesizing coordination-driven supramolecular constructs,^{7–15} the WLA is unique for its modular and convergent synthesis of multicomponent assemblies that can be predictably and reversibly toggled between multiple configurations in response to the

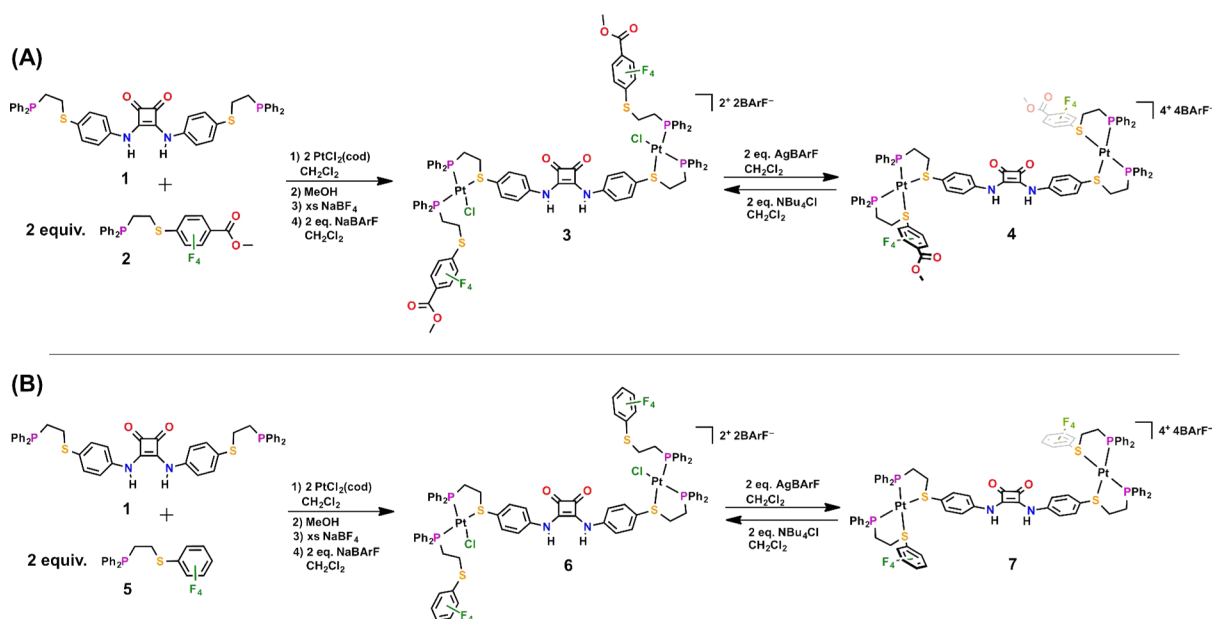
Received: August 26, 2014

Published: November 12, 2014

Scheme 1. Proposed Weak-Link Approach Triple-Decker Complex for the Allosteric Regulation of Squaramide Catalytic Activity^a

^aThe red circle represents catalytic feedstock, and the blue triangle represents catalytic product.

Scheme 2. (A) Synthesis of and Reversible Toggling between Flexible, Semiopen (3) and Rigid, Fully Closed (4) Configurations, and (B) Synthesis of and Reversible Toggling between Model Semiopen (6) and Model Fully Closed (7) Configurations



recognition of small-molecule effectors at chemically orthogonal regulatory sites.^{5,16–19} This is achieved via reversible coordination of small-molecule effectors (e.g., Cl[−], CO) to d⁸ metal-based structural nodes (e.g., Rh(I), Pt(II)), coordinated by phosphino–heteroatom (P,X; X = S, O, Se, N) hemilabile ligands. Therefore, we designed a heteroligated Pt(II) triple-decker complex featuring both a symmetric, homoditopic P,S-functionalized biphenylene squaramide HBD ligand (1), and two monotopic P,S-functionalized methyl tetrafluorobenzoate HBA ligands (2) (Scheme 2A). As we have previously demonstrated, utilizing a 2:2:1 mixture of PtCl₂(cod) and

two model P,S hemilabile ligands of significantly different chelating strength (e.g., P,S-tetrafluorophenyl and P,S-phenyl) affords the near-quantitative synthesis of a heteroligated Pt(II) triple-decker complex via the halide-induced ligand rearrangement reaction (HILR).²⁰ The hemilabile nature of the P,S-fluorophenyl motifs allows for the quantitative in situ conversion of the complex between a flexible, semiopen configuration and a rigid, geometrically constrained fully closed configuration. We predicted that in the semiopen state (3) intermolecular hydrogen-bonding interactions between the HBA ester moieties and the HBD squaramide moiety would

drive complex oligomerization analogous to enzymatic quaternary structure (Scheme 1). This extended hydrogen-bonding network would effectively outcompete substrate recognition, thus hampering catalytic activity. Upon in situ switching to the rigid, fully closed configuration (4), intermolecular ester–squaramide hydrogen-bonding would be disrupted by geometric and steric restraints, resulting in the stabilization of the monomeric state. Additionally, the tertiary structure would be such that the squaramide moiety is free to hydrogen-bonding to potential HBA substrates and activate them toward nucleophilic attack. To understand the differences in shape and structure between semiopen 3 and fully closed 4, as well as develop structure–function relationships, computational models were generated and optimized using DFT. Characterization of intermolecular hydrogen-bonding and complex oligomerization was performed using FT-IR spectroscopy concentration gradient studies and ^1H diffusion-ordered NMR spectroscopy (DOSY), respectively. The HBA substrate recognition capabilities of the two distinct states were studied using ^1H NMR spectroscopy substrate binding studies. Finally, to test the validity of our hypothesis, the ability of the WLA construct to allosterically regulate the Friedel–Crafts (F-C) reaction of indole and nitrostyrene in situ was determined. In addition to the functional complex, a model system was synthesized, possessing a simple proton in place of the HBA methyl ester moiety (Scheme 2B). These models were used as a control throughout this study to directly determine the role of intermolecular hydrogen-bonding in the regulatory mechanism.

RESULTS AND DISCUSSION

Synthesis. In order to create a supramolecular complex in which ligand–ligand hydrogen-bonding regulates the catalytic activity of a HBD catalyst (e.g., biphenylene squaramide),^{21,22} we designed a structure in which the two conformational states of the complex promote significantly disparate degrees of intermolecular interaction. Whereas the flexibility of monodentate ligands in the semiopen state would readily allow for intermolecular hydrogen-bonding, the fully closed configuration had to be properly designed to utilize geometric, steric, and, potentially, electrostatic restraints to limit ligand–ligand interactions. Previously, we reported on the single-crystal X-ray diffraction structures of both the semiopen and fully closed Pt(II) triple-decker model complexes.²⁰ Using these structures as an operational reference, we designed the aforementioned triple-decker complex, for which we expected the steric bulk associated with the “dumbbell-like” architecture of the fully closed state, combined with the rigid nature of the bidentate ligands and the tetravalent nature of the complex, to hinder hydrogen-bonding between the HBD and HBA ligands.

To afford the designed triple-decker complex, we utilized an adaptation of our previously reported syntheses for heteroligated Pt(II) complexes.²⁰ Specifically, 1 equiv of the bridging homoditopic P,S-functionalized biphenylene squaramide ligand (1) and 2 equiv of the monotopic P,S-functionalized methyl tetrafluorobenzoate ligand (2) were added to 2 equiv of Pt(II) precursor $\text{PtCl}_2(\text{cod})$. Upon isolation of semiopen 3 (BF_4), a counteranion exchange with NaBARF was performed, yielding divalent semiopen 3 (BARF). Utilizing BARF^- as the counteranion is critical for solubility in nonpolar solvents, which promote the catalytic activity of HBD catalysts. $^{31}\text{P}\{^1\text{H}\}$ NMR spectroscopy of semiopen 3 displays two resonances: one at 8.39 ppm ($J_{\text{P-P}} = 14$ Hz, $J_{\text{P-Pt}} = 3231$ Hz) corresponding to the P-bound P,S-fluorophenylene ligands, and the other at 43.44

ppm ($J_{\text{P-P}} = 14$ Hz, $J_{\text{P-Pt}} = 3466$ Hz), arising from the chelated P,S-phenylene squaramide-containing ligand. These values are in strong agreement with previously reported values for semiopen heteroligated Pt(II) structures.²⁰ Fully closed 4 can be isolated via two routes: (1) abstraction of inner-sphere chlorides from semiopen 3 (BF_4) with 2 equiv of AgBF_4 , followed by a counteranion exchange with NaBARF, or (2) abstraction of inner-sphere chlorides from semiopen 3 (BARF) via the addition of 2 equiv of a 0.1 M ethereal solution of AgBARF . The $^{31}\text{P}\{^1\text{H}\}$ NMR spectrum of fully closed 4 shows two downfield resonances at 44.57 ppm ($J_{\text{P-Pt}} = 3087$ Hz) and 45.79 ppm ($J_{\text{P-Pt}} = 3244$ Hz), corresponding to the fully chelated heteroligated configuration. Based on their corresponding P–Pt coupling constants, we can assign the resonance at 44.57 ppm to the phosphorus atom of the P,S-fluorophenylene ester-functionalized ligands (2), and the resonance at 45.79 ppm to the phosphorus atom of the symmetric P,S-phenylene squaramide bridging ligand (1). Both semiopen 3 and fully closed 4 are stable under ambient benchtop conditions.

DFT Calculations. To gain further insight into the structural organization of the synthesized structures, Density Functional Theory (DFT) calculations were used to generate models of the semiopen (3) and fully closed (4) states. Using the same parameters (GGA:PBE TZ2P) we have previously used to calculate the energy-minimized structures of heteroligated WLA complexes,^{23,24} we calculated the structures of 3 and 4. As can be seen in Figure 1A,B, both the ball-and-stick

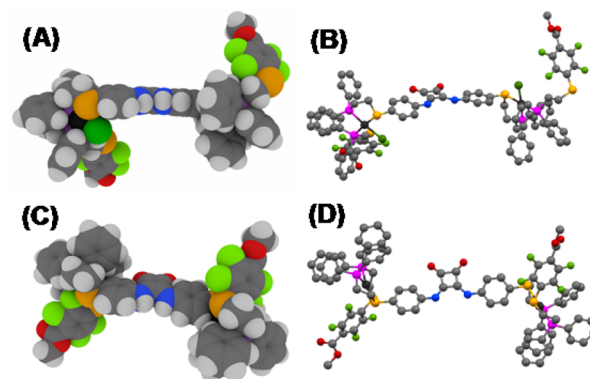


Figure 1. Energy-minimized structures: (A) space-filling front-on view of semiopen 3, (B) ball-and-stick front-on view of semiopen 3, (C) space-filling front-on view of fully closed 4, and (D) ball-and-stick top-down view of fully closed 4. Colors: C, gray; P, magenta; S, orange; O, red; N, blue; Pt, black; F, lime green; Cl, forest green; H, white. Hydrogens omitted from ball-and-stick structures for clarity.

and space-filling structures of semiopen 3 suggest that there are no geometric or steric constraints that would prevent the intermolecular hydrogen-bonding association of multiple semiopen complexes in solution. On the other hand, the geometry optimization of fully closed 4 (Figure 1C,D) shows a rigid, anisotropic “dumbbell-like” structure. This structure displays geometric rigidity of the ester ligands imposed by chelation, as well as the significant steric bulk of the end groups, which may cooperatively deter intermolecular association of the fully closed complexes.

Intermolecular Hydrogen-Bonding. In order to correlate the structural modeling to function, we needed to directly measure the self-associative behavior of the semiopen (3) and fully closed (4) configurations in solution. Previously, we have

demonstrated the ability to characterize hydrogen-bonding of urea derivatives in a WLA architecture using FT-IR spectroscopy by examining the N–H bond vibration that occurs from 3400 to 3200 cm^{-1} .²⁵ Unfortunately, the N–H bond vibration of diphenyl squaramide derivatives occurs between 3200 and 3000 cm^{-1} , thus overlapping with aliphatic and aromatic C–H bond stretches. Therefore, we turned to the less prominent C=O bond vibration of the squaramide backbone to characterize the degree of hydrogen-bonding in our structures. Through extensive efforts by de Oliveira et al., it has been shown that the C=O bond vibration of a diphenyl squaramide derivative occurs at approximately 1795 cm^{-1} .^{26,27} It was also computationally demonstrated that upon hydrogen-bond donation by the N–H moiety, the C=O bond vibration shifts to lower wavenumbers. Several computational investigations of diphenyl squaramide derivatives have concluded that the squaramide moiety is partially aromatic.²⁸ Therefore, the donation of electron density into the squaramide moiety via hydrogen-bonding to some electron-rich HBA moiety will increase the aromatic nature of the squaramide moiety. Such an increase in the conjugation of a C=O bond is well known to cause carbonyl bond vibrations to shift to lower wavenumbers.²⁹ Thus, to study the propensity of the complexes to form intermolecular hydrogen bonds between the ester and squaramide ligands we performed a FT-IR spectroscopy concentration gradient study in which the position of the C=O band was measured across a concentration range. As can be seen in Figure 2, increasing the concentration of semiopen 3

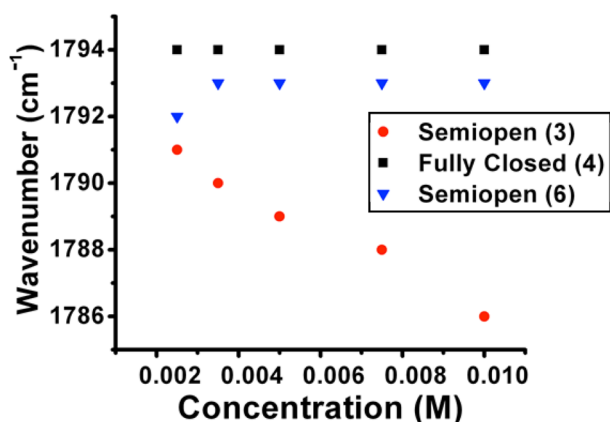


Figure 2. Wavenumber (cm^{-1}) of squaramide C=O bond vibration vs complex concentration in CH_2Cl_2 for semiopen 3 (red circle), fully closed 4 (black square), and ester-free semiopen model 6 (blue triangle).

from 0.0025 to 0.01 M in dichloromethane results in an approximately linear shift to lower wavenumbers. This trend suggests the presence of intermolecular hydrogen-bonding at the squaramide moiety. In contrast, there is no such shift in the C=O band of the fully closed complex (4) (Figure 2), suggesting negligible hydrogen-bonding interaction between the ester and squaramide moieties. In order to confirm that the observed trend for semiopen 3 is in fact due to hydrogen-bonding between the ester and squaramide moieties, the same experiment was performed with model semiopen 6. Indeed, the C=O bond vibration of model semiopen 6 does not shift with increasing concentration (Figure 2), confirming the intermolecular hydrogen-bonding interaction between the ester and squaramide moiety for semiopen 3. From these observations,

we can conclude that whereas the flexible, semiopen state (3) can form intermolecular hydrogen bonds, there is minimal interaction in the rigid, fully closed configuration (4). To our knowledge, this is the first example of direct characterization of hydrogen-bonding of a diphenyl squaramide HBD catalyst. It should be noted that no study of a mixture of the two free ligands in solution could be performed due to the complete insolubility of the free diphenylene squaramide ligand in any solvent in which there is negligible hydrogen-bonding interaction between solvent and squaramide.

Complex Oligomerization. Having characterized the significant difference in intermolecular hydrogen-bonding interactions, we sought to determine whether the coordination mode at the Pt(II) structural node controlled the quaternary structure of the construct. ^1H diffusion-ordered NMR spectroscopy (DOSY) was employed to determine the relative state of aggregation of 3 and 4. Recently, DOSY has become a powerful tool for characterizing noncovalent aggregates of supramolecular architectures and determining the degree of oligomerization.^{30–32} Therefore, ^1H DOSY experiments were run on both semiopen 3 (Figure 3) and fully closed complex 4,

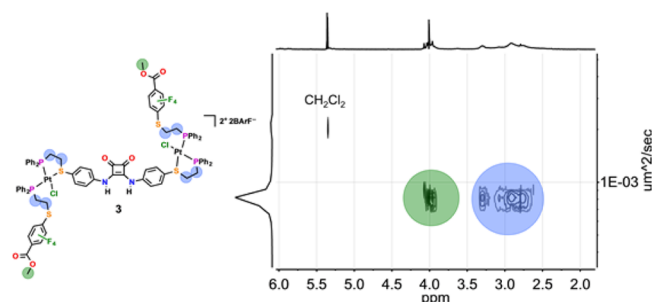


Figure 3. ^1H DOSY spectrum of semiopen 3 with CH_2Cl_2 as internal standard. Methyl protons of 3 are highlighted in green; ethylene protons of 3 are highlighted in blue.

as well as on their respective models (6 and 7), at 0.01 M concentration in dichloromethane. In order to determine the degree of oligomerization of the two configurations, the hydrodynamic volume (V_H) of the functional complexes, as determined by ^1H DOSY, were compared to that of their respective model complex.³⁰ Using this method, the V_H of semiopen 3 was calculated to be approximately four times greater than the V_H of model semiopen 6. Thus, assuming the model 6 is monomeric in solution, our study suggests that semiopen 3 exists as a tetramer in solution. In contrast, the V_H of fully closed 4 is approximately equal to that of its respective model complex, suggesting that fully closed 4 is monomeric. Alternatively, we can make a direct comparison of semiopen 3 and fully closed 4 by accounting for the apparent rigid structural anisotropy of 4, determined from the energy-minimized structure, in our calculation of V_H (see SI).³⁰ We thus derive a V_H ratio of approximately 5:1 for semiopen 3:fully closed 4. We attribute the deviation in the calculated state of aggregation between four and five to our inability to mathematically account for the difference in valency between the semiopen and fully closed states. Importantly, we can conclude that, at the given concentration in nonpolar solvent, the prevalence of intermolecular hydrogen-bonding in the flexible, semiopen state (3) drives oligomerization. Comparatively, fully closed 4 exists in a monomeric state.

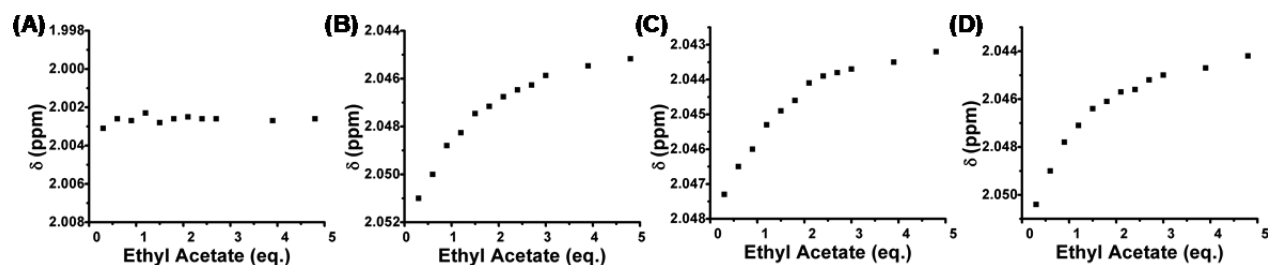


Figure 4. δ (ppm) of ethyl acetate methyl protons vs equivalents of ethyl acetate added to (A) semiopen 3, (B) fully closed 4, (C) ester-free model semiopen 6, and (D) ester-free model fully closed 7. Titrations performed with 1.2 mM solution of complex in CD_2Cl_2 .

HBA Substrate Association Studies. To evaluate the effects that toggling intermolecular hydrogen-bonding has on the HBA substrate recognition properties of semiopen 3 and fully closed 4, the respective complexes were titrated with ethyl acetate. Recognition was measured from the changes in ^1H NMR chemical shifts of the ethyl acetate methyl protons as a function of ethyl acetate equivalents added. Figure 4A shows negligible recognition of ethyl acetate by semiopen 3, even at high equivalency of the substrate. This is remarkable, as ethyl acetate is a more electron rich HBA substrate than the methyl fluorobenzoate ligand. We attribute this effect to the high local concentration of the HBA ligand around the HBD squaramide. In contrast, fully closed 4 displays significant substrate recognition (Figure 4B). Substrate recognition studies were also performed with glutaric anhydride and nitromethane. These substrates show the same “on–off” contrast in binding between the two complexes (see SI). Additional ethyl acetate titration studies were performed with the model semiopen (6) and fully closed (7) structures (Figure 4C,D). Both models show very similar binding curves to fully closed 4. From these studies we can infer a few points. First, intermolecular hydrogen-bonding interactions between the diphenylene squaramide and ester ligands in semiopen 3 prevent HBA substrate recognition. Second, in fully closed 4 the tertiary structure is such that the squaramide moiety is unimpeded by intermolecular hydrogen-bonding, thus available to bind HBA substrate. While geometric and steric restraints prevent ligand–ligand association, the adopted structure also exposes the squaramide active site. Third, there is no appreciable interaction between the HBD and HBA ligands in fully closed 4, as the substrate binding is very similar to the ester-free fully closed model 7.

Allosteric Regulation of Catalysis. Upon elucidating the significant differences in the quaternary and tertiary structures of semiopen 3 and fully closed 4, we tested whether these differences would translate into a significant difference in the catalytic activity of the diphenylene squaramide active site. Thus, we compared the ability of semiopen 3, fully closed 4, and semiopen model 6 to catalyze the C–C bond-forming F–C reaction between indole and nitrostyrene to form 3-(2-nitro-1-phenylethyl)-1H-indole (Figure 5A).^{33–37} The Lewis acid-catalyzed F–C addition of indole to nitroalkenes is the key initial step in the synthesis of many pharmacologically active alkaloid derivatives containing the tryptamine backbone.³⁸ The test reactions were carried out with a 1.5:1 indole:nitrostyrene stoichiometric ratio (0.03 M: 0.02 M) in 1,2-dichlorobenzene- d_4 at 60 °C, in the presence of 20 mol % of complex. All catalysis was performed under ambient, benchtop conditions. As seen in Figure 5B, semiopen complex 3 produces a negligible amount of product after 24 h, and in fact shows no

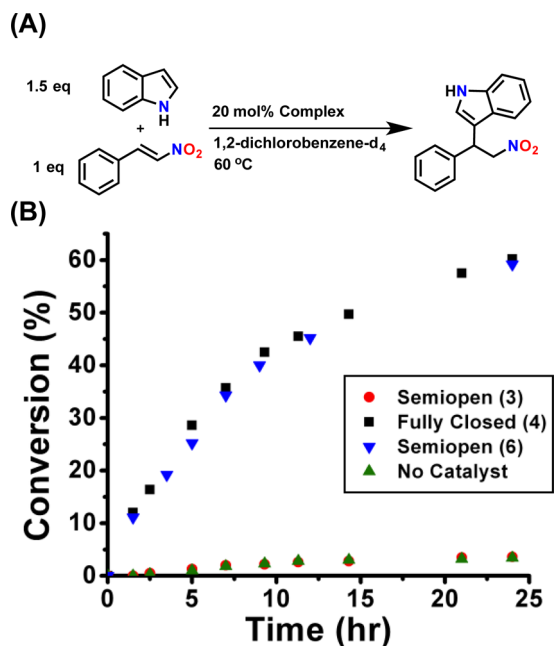


Figure 5. (A) Friedel–Crafts reaction between indole and nitrostyrene. (B) Fully closed 4 and ester-free semiopen model 6 show rate acceleration. Semiopen 3 shows no activity relative to catalyst free control. Reaction progress was monitored by ^1H NMR spectroscopy. Conditions were the following: 1.5:1 indole:nitrostyrene (0.03 M: 0.02 M), 60 °C, 1,2-dichlorobenzene- d_4 , 20 mol % complex.

activity relative to the catalyst-free control ($\text{TOF} = 1.74 \times 10^{-6} \text{ s}^{-1}$). Comparatively, fully closed 4 shows significant rate acceleration and catalytic turnover, with a turnover frequency of $3.47 \times 10^{-5} \text{ s}^{-1}$, approximately 21.5 times that of semiopen 3. Model semiopen complex 6 shows very similar rate acceleration to fully closed 4. These results confirm that by regulating oligomerization and substrate recognition via control of competitive hydrogen-bonding events, we can control the catalytic activity of the diphenylene squaramide moiety.

With the significant difference in activity between the two configurations, we investigated the ability to allosterically regulate catalytic activity in situ in the presence of the substrates. Therefore, using the same conditions described above, fully closed complex 4 was allowed to catalyze the F–C reaction for 2 h, after which 2 equiv of $\text{N}(\text{Bu})_4\text{Cl}$ were added to the reaction solution. Upon the formation of the semiopen complex 3, catalytic activity became negligible (Figure 6). After 2 h, during which no product was formed, fully closed 4 was re-formed in situ via the addition of 2 equiv of AgBARF .³⁹ After a short dative period, the F–C reaction is re-initiated (Figure 6). Therefore, by reversibly controlling the coordination mode of

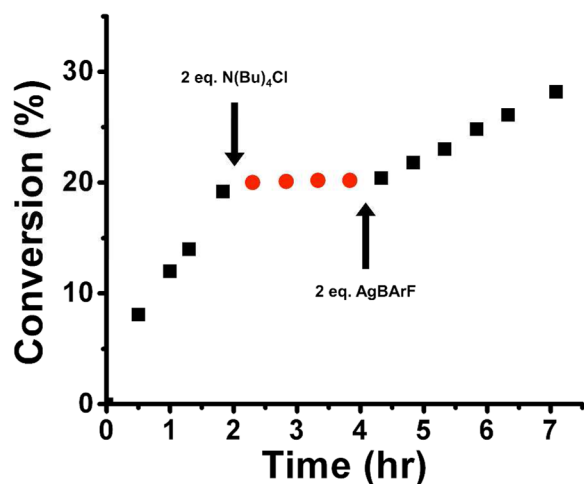


Figure 6. In situ addition of 2 equiv of $N(Bu)_4Cl$ after 2 h to a solution of fully closed **4**, catalyzing the Friedel–Crafts reaction between indole and nitrostyrene, shows immediate turn-off of catalysis, due to formation of semiopen **3**. In situ re-formation of **4** and re-initiation of activity achieved by the addition of 2 equiv of $AgBARF$.

the structural center, the ability of the diphenylene squaramide site to catalyze the targeted reaction is allosterically regulated. We hypothesize that the observed reduction in rate upon re-initiating catalysis is due to the depletion of the catalytic feedstock. This is the first example of allosteric regulation of catalytic activity using a WLA construct under benchtop conditions. Indeed, by controlling the effective quaternary and tertiary structure the HBD squaramide-containing triple-decker complex, we have developed a novel approach to reversible regulation of catalytic activity in situ.

CONCLUSION

In using intermolecular hydrogen-bonding to regulate the catalytic activity of a supramolecular construct, we have developed a novel synthetic analogue of a key enzymatic allosteric mechanism. Using the weak-link approach, we were able to design and synthesize a supramolecular assembly with predictable structural geometry, giving precise control of hydrogen-bonding interactions. The hemilabile nature of the phosphino–thioether ligands used to assemble the triple-decker construct allows for the reversible in situ switching between a flexible, oligomerized semiopen state and a rigid, monomeric fully closed state. By doing so, we were able to mimic Nature's ability to reversibly affect the quaternary structure of metabolically important enzymes. Additionally, these changes in quaternary structure coincide with changes in the tertiary structure of the squaramide active site, manifested as a drastic difference in catalytic activity. In contrast with previous allosterically regulated WLA complexes, the complex herein is catalytically dormant in the semiopen state, and active in the fully closed state. This reversal of the structure–function relationship opens doors to utilizing multiple WLA complexes simultaneously in situ for small-molecule-regulated cascade-like reaction pathways. The ability to precisely and simultaneously control the activity of multiple orthogonal catalysts with simple small-molecule effectors in situ would be unprecedented. Additionally, this work sets the stage for the allosteric regulation of functional WLA hydrogen-bonding-driven polymeric materials. Such stimuli responsive polymeric materials could have significant applications in signal detection and

amplification. Moving forward we plan to incorporate enantiomeric Lewis base cocatalysts into the WLA structure to expand the catalogue of applicable and controllable reactions catalyzed by HBD catalysts.

EXPERIMENTAL SECTION

General Methods. Phosphino–thioether ligands **1**, **2**, and **5**, and precursors were prepared and stored using standard Schlenk line techniques under an inert nitrogen atmosphere, unless noted otherwise. Ligand **5** was prepared as previously reported.⁴⁰ Ligand precursor 1-chloro-2-(diphenylphosphino)ethane was prepared as previously reported.¹⁹ The synthesis of Pt(II) complexes, **3**, **4**, **6**, and **7**, and their manipulations and characterization, were performed under ambient conditions. All solvents used for ligand and complex synthesis were anhydrous grade, purchased from Sigma-Aldrich. Deuterated solvents were purchased from Cambridge Isotope Laboratories and used as received. All other chemicals were purchased from Aldrich Chemical Co. and used as received. 1H NMR spectra were recorded on a Bruker Avance III 400 MHz spectrometer. 1H NMR spectra were referenced internally to residual protons in the deuterated solvents (dichloromethane- d_2 : δ 5.32 ppm, dimethylsulfoxide- d_6 : δ 2.50 ppm). $^{31}P\{^1H\}$ NMR spectra were referenced to an external 85% H_3PO_4 standard (δ 0 ppm). $^{19}F\{^1H\}$ NMR spectra were referenced to an external $CFCl_3$ standard (δ 0 ppm). Electrospray ionization (ESI) mass spectra were recorded on a Bruker AmaZon SL LC–MS instrument in positive ion mode.

Synthesis. 4-(2-Diphenylphosphanylethylthio)phenylamine. 1-Chloro-2-(diphenylphosphino)ethane (3.00 g, 12.06 mmol) and 4-aminothiophenol (1.50 g, 12.06 mmol) were dissolved in degassed anhydrous acetonitrile (15 mL) in an oven-dried Schlenk flask. With stirring, cesium carbonate (3.93 g, 12.06 mmol) was added, and the reaction mixture was heated to reflux for 12 h under nitrogen. After cooling to room temperature, the mixture was filtered through a glass frit, and the retentate was washed with acetonitrile. The solvent was removed from the filtrate under reduced pressure. Silica-gel column chromatography (dichloromethane) afforded the product as an off-white solid (2.84 g, 70% yield). 1H NMR (400.16 MHz, 25 °C, CD_2Cl_2): δ 7.41–7.35 (m, 10H), 7.22 (d, J_{H-H} = 8 Hz, 2H), 6.72 (d, J_{H-H} = 8 Hz, 2H), 4.82 (br s, 2H), 2.85 (m, 2H), 2.31 (m, 2H). $^{31}P\{^1H\}$ NMR (161.94 MHz, 25 °C, CD_2Cl_2): δ –17.54 (s, 1P). ESI-MS (m/z): 337 [M]⁺. Found 337.

3,4-((2-Diphenylphosphanylethylthio)phenylamino)cyclobut-3-ene-1,2-dione (**1**). To an anhydrous mixture of toluene:dimethylformamide (19:1, 7 mL) were added 3,4-dimethoxycyclobut-3-ene-1,2-dione (dimethyl squarate) (200 mg, 1.41 mmol) and zinc trifluoromethanesulfonate (102.6 mg, 0.28 mmol). The suspension was stirred vigorously for 10 min at room temperature. To the mixture was added 4-(2-diphenylphosphanylethylthio)phenylamine at once (1.00 g, 2.96 mmol). The mixture was heated to 100 °C and stirred overnight. The reaction was cooled to room temperature and filtered. The retentate was washed with toluene, methanol, and hexanes. The solid was dried to give a yellow solid (775 mg, 73% yield). 1H NMR (400.16 MHz, 25 °C, DMSO- d_6): δ 9.90 (br s, 2H), 7.42 (d, J_{H-H} = 8 Hz, 4H), 7.38–7.37 (m, 10H), 7.26 (d, J_{H-H} = 8 Hz, 4H), 2.92 (m, 4H), 2.33 (m, 4H). $^{31}P\{^1H\}$ NMR (161.94 MHz, 25 °C, DMSO- d_6): δ –17.51 (s, 2P).

(2-Diphenylphosphanylethylthio)triisopropylsilane (*P,S*-TIPS). To a dry, degassed 500 mL Schlenk flask was added 150 mL of dry THF, and then 100 mL of 0.5 M $KPPH_2$ (50 mmol) was cannulated into the flask. The solution was cooled in an ice bath. Ethylene sulfide (3.27 mL, 55 mmol) was added dropwise and stirred for 10 min at 0 °C. Triisopropylsilyl chloride (10.7 mL, 50 mmol) was added slowly dropwise. The reaction was stirred for 2 h. (Additional dry THF was added if reaction congealed.) The solvent was removed under reduced pressure, giving a gray oil. The crude mixture was extracted into the organic phase using a CH_2Cl_2 :water mixture (3 \times). The organic phase was dried with magnesium sulfate, and then the drying agent was removed by filtering through a fritted funnel. CH_2Cl_2 was removed under reduced pressure. The crude oil was purified using silica-gel

chromatography (2:1 hexanes:CH₂Cl₂), affording a colorless, crude oil (7.02 g, 34% yield). ¹H NMR (400.16 MHz, 25 °C, CD₂Cl₂): 7.47–7.38 (m, 10H), 2.59 (m, 2H), 2.39 (m, 2H), 1.16 (m, 3H), 1.07 (d, J_{H–H} = 8 Hz, 18H). ³¹P{¹H} NMR (161.94 MHz, 25 °C, CD₂Cl₂): δ –16.08 (s, 1P). ESI-MS (*m/z*): 402.65 [M]⁺. Found 403.65.

Methyl (2-Diphenylphosphanylethylthio)-2,3,5,6-tetrafluorobenzoate (2). To minimal dry, degassed DMF in a Schlenk flask were added P,S-TIPS (1.00 g, 2.48 mmol) and methyl pentafluorobenzoate (0.36 mL, 2.48 mmol). The solution was stirred for 10 min. Cesium fluoride (376 mg, 2.48 mmol) was added, and the reaction was stirred overnight at room temperature. The solvent was removed under reduced pressure. The crude was extracted with CH₂Cl₂:water (3 × 50 mL CH₂Cl₂). The organic phase was dried with magnesium sulfate and then filtered through a fritted funnel. CH₂Cl₂ was removed under reduced pressure giving a yellow oil, which upon drying on the high-vacuum line yielded **2** as a pale yellow solid (1.07 g, 95% yield). If need be, **2** can be purified by silica-gel chromatography (1:1 hexanes:CH₂Cl₂). ¹H NMR (400.16 MHz, 25 °C, CD₂Cl₂): δ 7.44–7.37 (m, 10H), 4.00 (s, 3H), 3.09 (m, 2H), 2.37 (m, 2H). ³¹P{¹H} NMR (161.94 MHz, 25 °C, CD₂Cl₂): δ –17.35 (s, 1P). ¹⁹F {¹H} NMR (376.49 MHz, 25 °C, CD₂Cl₂): δ –133.73 (m, 2F), –139.86 (m, 2F). ESI-MS (*m/z*): 452.06 [M]⁺. Found 453.06.

Semiopen Complex (BARF)₂ (3). A solution of PtCl₂(cod) (150 mg, 0.40 mmol) in CH₂Cl₂ (20 mL) was added dropwise to a CH₂Cl₂ slurry of **1** (150.9 mg, 0.20 mmol). To this mixture was added, dropwise, a solution of **2** (181.4 mg, 0.40 mmol) in CH₂Cl₂ (5 mL). The resulting solution was stirred for 15 min. MeOH (15 mL) was added, and the CH₂Cl₂ was removed under reduced pressure. An additional 150 mL of MeOH was added, and the solution was stirred overnight. The MeOH was reduced under reduced pressure to 1/10th the volume. To the MeOH solution was added a methanolic solution (5 mL) of excess NaBF₄ (65.8 mg, 0.60 mmol). The solution was stirred overnight and then filtered over a fritted funnel. The retentate was washed with minimal cold MeOH and then hexanes, yielding a yellow solid (3(BF₄)₂). The yellow solid was dried under vacuum overnight. The resulting yellow solid was added to a solution of 2 equiv of NaBARF in CH₂Cl₂ (10 mL) and then stirred overnight. The resulting slurry was filtered over Celite on a fritted funnel and then washed with dry CH₂Cl₂. The filtrate was collected, and the CH₂Cl₂ was removed under reduced pressure to yield **3** (550 mg, 72% yield). ¹H NMR (400.16 MHz, 25 °C, CD₂Cl₂): δ 7.71 (s, 16H), 7.63 (br m, 10H), 7.54 (s, 8H), 7.46 (br m, 20H), 7.26 (br m, 20H), 3.97 (s, 6H), 3.22–2.70 (br m, 16H). ³¹P{¹H} NMR (161.98 MHz, 25 °C, DMSO-*d*₆): δ 43.44 (d, J_{P–P} = 14 Hz, J_{P–Pt} = 3466 Hz, 2P), 8.39 (d, J_{P–P} = 14 Hz, J_{P–Pt} = 3231 Hz, 2P). ESI-MS (*m/z*): 1058.09 [M – 2BARF]²⁺. Found 1059.49.

Fully Closed Complex (BARF)₄ (4). **4** was synthesized via two methods: (a) abstraction of 3(BF₄)₂ in nitromethane with AgBF₄, followed by a counteranion exchange with NaBARF in CH₂Cl₂, and (b) abstraction of **3** in CH₂Cl₂ with an ethereal solution of AgBARF.

Method (a). To a solution of 3(BF₄)₂ (250 mg, 0.11 mmol) in nitromethane (10 mL) was added 2 equiv of AgBF₄ (42.8 mg, 0.22 mmol). The solution was stirred overnight occluded from light. The resulting slurry was filtered through Celite on a fritted funnel. The Celite was washed with dry CH₂Cl₂. The filtrate was collected, and then the CH₂Cl₂ was minimized under reduced pressure. Hexanes (20 mL) was added, and the suspension was stored at –20 °C for 1 h. The suspension was filtered over a fritted funnel, and then washed with hexanes. The yellow retentate was dried overnight. The resulting yellow solid was added to a solution of 4 equiv of NaBARF in CH₂Cl₂ and then stirred overnight. The resulting suspension was filtered over Celite on a fritted funnel, and the Celite was washed with dry CH₂Cl₂. The filtrate was collected, and the CH₂Cl₂ was removed under reduced pressure, giving a yellow oil. The oil was dried under high vacuum to give yellow solid **4** (531 mg, 88% yield).

Method (b). To a CH₂Cl₂ solution of **3** (100 mg, 0.026 mmol) was added 2 equiv of a 0.1 M ethereal solution of AgBARF.³⁹ The solution was stirred overnight occluded from light. The resulting suspension was filtered over Celite on a fritted funnel. The Celite was washed with dry CH₂Cl₂. The filtrate was collected, and the CH₂Cl₂ was removed

under reduced pressure, giving a yellow oil. The oil was dried under high vacuum to give yellow solid **4** (134 mg, 94% yield). ¹H NMR (400.16 MHz, 25 °C, CD₂Cl₂): δ 7.75 (s, 32 H), 7.66 (br m, 10H), 7.57 (s, 16H), 7.50 (br m, 20H), 7.35 (br m, 20H), 3.95 (s, 6H), 3.15–2.90 (br m, 16H). ³¹P{¹H} NMR (161.98 MHz, 25 °C, DMSO-*d*₆): 45.79 (br s, J_{P–Pt} = 3244 Hz, 2P), 44.57 (br s, J_{P–Pt} = 3087 Hz, 2P). ESI-MS (*m/z*): 682.61 [M – 4BARF]³⁺. Found 681.98.

Semiopen Complex (BARF)₂ (6). A solution of PtCl₂(cod) (150 mg, 0.40 mmol) in CH₂Cl₂ (20 mL) was added dropwise to a CH₂Cl₂ slurry of **1** (150.9 mg, 0.20 mmol). To this mixture was added, dropwise, a solution of **5** (157.7 mg, 0.40 mmol) in CH₂Cl₂ (5 mL). The resulting solution was stirred for 15 min. MeOH (15 mL) was added, and the CH₂Cl₂ was removed under reduced pressure. An additional 150 mL of MeOH was added, and the solution was stirred overnight. The MeOH was reduced under reduced pressure to 1/10th the volume. To the MeOH solution was added a methanolic solution (5 mL) of excess NaBF₄ (65.8 mg, 0.60 mmol). The solution was stirred overnight and then filtered over a fritted funnel. The retentate was washed with minimal cold MeOH and then hexanes, yielding a yellow solid (6(BF₄)₂). The yellow solid was dried under vacuum overnight. The resulting yellow solid was added to a solution of 2 equiv of NaBARF in CH₂Cl₂ (10 mL) and then stirred overnight. The resulting slurry was filtered over Celite on a fritted funnel and then washed with dry CH₂Cl₂. The filtrate was collected, and the CH₂Cl₂ was removed under reduced pressure to yield **6** (564 mg, 76% yield). ¹H NMR (400.16 MHz, 25 °C, CD₂Cl₂): δ 8.08 (m, 2H), 7.75 (s, 16 H), 7.64 (br m, 8H), 7.58 (s, 8H), 7.49 (br m, 20H), 7.28 (br m, 20H), 3.00–2.20 (br m, 16H). ³¹P{¹H} NMR (161.98 MHz, 25 °C, DMSO-*d*₆): 43.72 (d, J_{P–P} = 15 Hz, J_{P–Pt} = 3540 Hz, 2P), 8.72 (d, J_{P–P} = 15 Hz, J_{P–Pt} = 3236 Hz, 2P). ESI-MS (*m/z*): 1017.57 [M + Cl[–] – 2BARF]¹⁺. Found 1018.97.

Fully Closed Complex (BARF)₄ (7). **7** was synthesized via two methods: (a) abstraction of 6(BF₄)₂ in nitromethane with AgBF₄, followed by a counteranion exchange with NaBARF in CH₂Cl₂, and (b) abstraction of **6** in CH₂Cl₂ with an ethereal solution of AgBARF.

Method (a). To a solution of 6(BF₄)₂ (216 mg, 0.1 mmol) in nitromethane (10 mL) was added 2 equiv of AgBF₄ (38.8 mg, 0.2 mmol). The solution was stirred overnight occluded from light. The resulting slurry was filtered through Celite on a fritted funnel. The Celite was washed with dry CH₂Cl₂. The filtrate was collected, and then the CH₂Cl₂ was minimized under reduced pressure. Hexanes (20 mL) was added, and the suspension was stored at –20 °C for 1 h. The suspension was filtered over a fritted funnel and then washed with hexanes. The yellow retentate was dried overnight. The resulting yellow solid was added to a solution of 4 equiv of NaBARF in CH₂Cl₂ and then stirred overnight. The resulting suspension was filtered over Celite on a fritted funnel, and the Celite was washed with dry CH₂Cl₂. The filtrate was collected, and the CH₂Cl₂ was removed under reduced pressure, giving a yellow oil. The oil was dried under high vacuum to give yellow solid **7** (461 mg, 86% yield).

Method (b). To a CH₂Cl₂ solution of **6** (100 mg, 0.027 mmol) was added 2 equiv of a 0.1 M ethereal solution of AgBARF.³⁹ The solution was stirred overnight occluded from light. The resulting suspension was filtered over Celite on a fritted funnel. The Celite was washed with dry CH₂Cl₂. The filtrate was collected, and the CH₂Cl₂ was removed under reduced pressure, giving a yellow oil. The oil was dried under high vacuum to give yellow solid **7** (132 mg, 92% yield). ¹H NMR (400.16 MHz, 25 °C, CD₂Cl₂): δ 8.08 (m, 2H), 7.75 (s, 32 H), 7.66 (br m, 8H), 7.57 (s, 16H), 7.51 (br m, 20H), 7.32 (br m, 20H), 3.92–2.13 (br m, 16H). ³¹P{¹H} NMR (161.98 MHz, 25 °C, DMSO-*d*₆): 45.04 (d, J_{P–P} = 13 Hz, J_{P–Pt} = 3250 Hz, 2P), 44.63 (d, J_{P–P} = 13 Hz, J_{P–Pt} = 3113 Hz, 2P).

■ ASSOCIATED CONTENT

§ Supporting Information

Details of computational geometry optimization, FT-IR study of self-association, ¹H DOSY study of oligomerization, ¹H NMR spectroscopy study of substrate binding and catalytic study, ³¹P{¹H} and ¹H NMR spectra of **1**, **3**, **4**, **6** and **7**, and

$^{31}\text{P}\{^1\text{H}\}$, ^1H and $^{19}\text{F}\{^1\text{H}\}$ NMR spectra of **2** and **5**. This material is available free of charge via the Internet at <http://pubs.acs.org>.

AUTHOR INFORMATION

Corresponding Author

chadnano@northwestern.edu

Notes

The authors declare no competing financial interest.

ACKNOWLEDGMENTS

This material is based upon work supported by awards from the National Science Foundation (CHE-1149314) and U.S. Army (W911NF-11-1-0229). J.M.-A. acknowledges a fellowship from Consejo Nacional de Ciencia y Tecnología (CONACYT).

REFERENCES

- (1) Traut, T. W. *Crit. Rev. Biochem. Mol. Biol.* **1994**, *29*, 125.
- (2) Barford, D.; Johnson, L. *Nature* **1989**, *340*, 609.
- (3) Ali, M. H.; Imperiali, B. *Bioorg. Med. Chem.* **2005**, *13*, 5013.
- (4) Goodey, N. M.; Benkovic, S. J. *Nat. Chem. Biol.* **2008**, *4*, 474.
- (5) Gianneschi, N. C.; Masar, M. S.; Mirkin, C. A. *Acc. Chem. Res.* **2005**, *38*, 825.
- (6) Oliveri, C. G.; Ulmann, P. A.; Wiester, M. J.; Mirkin, C. A. *Acc. Chem. Res.* **2008**, *41*, 1618.
- (7) Molenveld, P.; Engbersen, J. F. J.; Reinhoudt, D. N. *Chem. Soc. Rev.* **2000**, *29*, 75.
- (8) Prins, L. J.; Huskens, J.; de Jong, F.; Timmerman, P.; Reinhoudt, D. N. *Nature* **1999**, *398*, 498.
- (9) Lin, W. *Supramolecular Catalysis*; Wiley-VCH Verlag GmbH & Co. KGaA: Weinheim, 2008; p 93.
- (10) Lee, S. J.; Lin, W. *Acc. Chem. Res.* **2008**, *41*, 521.
- (11) Fujita, M.; Tominaga, M.; Hori, A.; Therrien, B. *Acc. Chem. Res.* **2005**, *38*, 369.
- (12) Ikemoto, K.; Inokuma, Y.; Fujita, M. *J. Am. Chem. Soc.* **2011**, *133*, 16806.
- (13) Caulder, D. L.; Raymond, K. N. *Acc. Chem. Res.* **1999**, *32*, 975.
- (14) Das, S.; Incarvito, C. D.; Crabtree, R. H.; Brudvig, G. W. *Science* **2006**, *312*, 1941.
- (15) Sauvage, J. P.; Collin, J. P.; Chambron, J. C.; Guillerez, S.; Coudret, C.; Balzani, V.; Barigelli, F.; De Cola, L.; Flamigni, L. *Chem. Rev.* **1994**, *94*, 993.
- (16) Farrell, J. R.; Mirkin, C. A.; Guzei, I. A.; Liable-Sands, L. M.; Rheingold, A. L. *Angew. Chem., Int. Ed.* **1998**, *37*, 465.
- (17) Gianneschi, N. C.; Bertin, P. A.; Nguyen, S. T.; Mirkin, C. A.; Zakharov, L. N.; Rheingold, A. L. *J. Am. Chem. Soc.* **2003**, *125*, 10508.
- (18) Holliday, B. J.; Mirkin, C. A. *Angew. Chem., Int. Ed.* **2001**, *40*, 2022.
- (19) Yoon, H. J.; Kuwabara, J.; Kim, J.-H.; Mirkin, C. A. *Science* **2010**, *330*, 66.
- (20) Kennedy, R. D.; Machan, C. W.; McGuirk, C. M.; Rosen, M. S.; Stern, C. L.; Sarjeant, A. A.; Mirkin, C. A. *Inorg. Chem.* **2013**, *52*, 5876.
- (21) Malerich, J. P.; Hagihara, K.; Rawal, V. H. *J. Am. Chem. Soc.* **2008**, *130*, 14416.
- (22) Alemán, J.; Parra, A.; Jiang, H.; Jørgensen, K. A. *Chem.—Eur. J.* **2011**, *17*, 6890.
- (23) Park, J. S.; Lifschitz, A. M.; Young, R. M.; Mendez-Arroyo, J.; Wasielewski, M. R.; Stern, C. L.; Mirkin, C. A. *J. Am. Chem. Soc.* **2013**, *135*, 16988.
- (24) Lifschitz, A. M.; Young, R. M.; Mendez-Arroyo, J.; Roznyatovskiy, V. V.; McGuirk, C. M.; Wasielewski, M. R.; Mirkin, C. A. *Chem. Commun.* **2014**, *50*, 6850.
- (25) McGuirk, C. M.; Stern, C. L.; Mirkin, C. A. *J. Am. Chem. Soc.* **2014**, *136*, 4689.
- (26) Silva, C. E.; Dos Santos, H. I. F.; Speziali, N. L.; Diniz, R.; de Oliveira, L. F. C. *J. Phys. Chem. A* **2010**, *114*, 10097.
- (27) Lunelli, B.; Giorgini, M. G. *Spectrochim. Acta A—M* **1988**, *44*, 1153.
- (28) Storer, R. I.; Aciro, C.; Jones, L. H. *Chem. Soc. Rev.* **2011**, *40*, 2330.
- (29) Wade, L. G., Jr. *Organic Chemistry*, 7th ed.; Prentice Hall: Upper Saddle River, NJ, 2010.
- (30) Macchioni, A.; Ciancaleoni, G.; Zuccaccia, C.; Zuccaccia, D. *Chem. Soc. Rev.* **2008**, *37*, 479.
- (31) Cohen, Y.; Avram, L.; Frish, L. *Angew. Chem., Int. Ed.* **2005**, *44*, 520.
- (32) Kapur, G. S.; Cabrita, E. J.; Berger, S. *Tetrahedron Lett.* **2000**, *41*, 7181.
- (33) Herrera, R. P.; Sgarzani, V.; Bernardi, L.; Ricci, A. *Angew. Chem., Int. Ed.* **2005**, *44*, 6576.
- (34) Ganesh, M.; Seidel, D. *J. Am. Chem. Soc.* **2008**, *130*, 16464.
- (35) da Silva, R. C.; da Silva, G. P.; Sangi, D. P.; Pontes, J. G. d. M.; Ferreira, A. G.; Corrêa, A. G.; Paixão, M. W. *Tetrahedron* **2013**, *69*, 9007.
- (36) Dessole, G.; Herrera, R. P.; Ricci, A. *Synlett* **2004**, *2004*, 2374.
- (37) Loh, C. C. J.; Atodiresi, I.; Enders, D. *Chem.—Eur. J.* **2013**, *19*, 10822.
- (38) Lancianesi, S.; Palmieri, A.; Petrini, M. *Chem. Rev.* **2014**, *114*, 7108.
- (39) Hayashi, Y.; Rohde, J. J.; Corey, E. J. *J. Am. Chem. Soc.* **1996**, *118*, 5502.
- (40) Brown, A. M.; Ovchinnikov, M. V.; Mirkin, C. A. *Angew. Chem., Int. Ed.* **2005**, *44*, 4207.